



# A series of spatio-temporal analyses and predicting modeling of land use and land cover changes using an integrated Markov chain and cellular automata models

Aqil Tariq<sup>1,2</sup> · Faisal Mumtaz<sup>3,4</sup>

Received: 20 May 2022 / Accepted: 31 January 2023 / Published online: 6 February 2023  
© The Author(s), under exclusive licence to Springer-Verlag GmbH Germany, part of Springer Nature 2023

## Abstract

For sustainable land cover planning, spatial land cover models are essential. Deforestation, loss of agriculture, and conversion of pasture land to urban and industrial uses are only some of the negative consequences of human kind's insatiable need for more land. Using remote sensing multi-temporal data, spatial criteria, and prediction models can effectively monitor these changes and plan for sustainable land use. This research aims to predict the land use and land cover (LULC) with cellular automata (CA) and Markov chain models. Landsat TM, ETM+, and OLI/TIRS data were used for mapping LULC distributions for the years 1990, 2006, and 2022. A CA-Markov chain was developed for simulating long-term landscape changes at 16-year time steps from 2022 to 2054. Analysis of urban sprawl was carried out by using the support vector machine (SVM). Through the CA-Markov chain analysis, we expect that built-up area will grow from 285.68 km<sup>2</sup> (22.59%) to 383.54 km<sup>2</sup> (30.34%) in 2022 and 2054, as inferred from the changes that occurred from 1990 to 2022. Therefore, substantial deforestation area reduction will result if existing tendencies in change continue despite sustainable development efforts. The findings of this research can inform land cover management strategies and assist local authorities in preparing for the present and the future. They can balance expanding the city and preserving its natural resources.

**Keywords** Cellular automata · Markov chain · Urbanization · Multi-criteria evaluation · SVM

## Introduction

Alterations to land use and land cover (LULC) have recently emerged as a topic of concern worldwide because of the impact these alterations have on the global system (Ghaffar et al. 2013; Hassan et al. 2016; Sarkar 2019). The term “land use” refers to the myriad ways in which land can be used to satisfy various human requirements. The essential criteria are having a thorough understanding of land use patterns, making the best possible use of available land, and being aware of how these aspects evolve through time. LULC transformation typically occurs in two manifestations, conversion and change (Owojori and Xie 2003). Alterations to the LULC significantly influence various impacts brought about by climate change (Owojori and Xie 2003; Khan et al. 2021).

The human factor degrades physical, ecological resources (e.g., water, soil, and air) and significantly affect environmental quality. As a result of human activity, changes have been observed in the dispersal of precipitation and the in land surface temperature (Wang et al. 2018) and LULC

---

Responsible Editor: Philippe Garrigues

✉ Aqil Tariq  
at2139@msstate.edu; aqiltariq@whu.edu.cn;  
aqiltariq85@gmail.com

<sup>1</sup> Department of Wildlife, Fisheries and Aquaculture, College of Forest Resources, Mississippi State University, 775 Stone Boulevard, Starkville, MS 39762-9690, USA

<sup>2</sup> State Key Laboratory of Information Engineering in Surveying, Mapping and Remote Sensing, Wuhan University, Wuhan 430072, Hubei, China

<sup>3</sup> State Key Laboratory of Remote Sensing Sciences, Aerospace Information Research Institute, Chinese Academy of Sciences, Beijing 100101, China

<sup>4</sup> University of Chinese Academy of Sciences (UCAS), Beijing 101408, China

resources on a local, regional, and global scale (Li et al. 2016; Hussain et al. 2022). (Erinjery et al. 2018) Increasing extremes, ecohydrological consequences (arid and semi-arid), disturbance of the groundwater hydraulic cycle and quality (Morshed and Fattah 2021), and Mitigation policies (Behera et al. 2012). Thus, a given location's biological, physical, and hydrological aspects interact in intricate ways to determine the quality of the land cover (Li et al. 2017). Monitoring the trajectory of changes necessitates an evaluation of the existing spatial and temporal dynamics of LULC to make more informed assessments in the future.

Rapid land use change affects more than just the surrounding countryside and city (Samanta et al. 2018). Over-use of LULC for a variety of political and economic ends has the potential to diminish the land's current and future usefulness. An excellent example of how the socio-economic aspects of land use change in agriculture become an urgent problem after drought impacts are followed by the construction of roads and public transit is the abandonment of land in rural areas as a result of residents' more accessible and faster migrations. As a result, new environmental and socio-economic concerns arise, including decreased productivity and unsustainable agricultural development, which have wide-ranging regional and temporal effects (Tulbure and Broich 2019). Farmers will abandon less land if the present LULC evaluation is accurate (Shao et al. 2019). However, urbanization and sprawl convert agricultural land to non-agricultural uses and put natural resources at risk (Mondal et al. 2022), which can lead to a decrease in rural resources (Kim and Brown 2021).

Predicting how land will be used accurately is crucial to evaluating the feasibility of standardizing and integrating data sets and creating maps. Logistic regression models have many advantages over other methods (combined with other models but do not clarify the relative importance of the motivating factors). The CA–Markov model is a hybrid that combines ideas from CA (an exposed formation that may be easily integrated with knowledge-driven models and the Markov chain model (accurate spatial and temporal modeling) (Tariq et al. 2022b). To build the Markov chain, we use a set of probability values that, based on historical data, depict the possibility of changing user interfaces through time. At any given time, a given area of the planet might theoretically shift from one category of land use to another (Atif et al. 2015). With the help of matrices, Markov chain analysis may examine the dynamics of all possible land use transitions across all likely display groups. Over the past three decades, the Markov chain model's precision and reliability have led to its widespread use in various LULC research (Tulbure and Broich 2019; Siddiqui et al. 2020; Roy et al. 2021, 2022; Yohannes et al. 2021). Transition probabilities of several land use interactions across time can be evaluated with CA–Markov. Due to these transitions between

sizes, one or more land uses can become dominant in a given area. In this technique, the number of pixels belonging to different land use classes at other times is represented by a matrix that shows the area's change over time. As stated in a Markov chain, coating types have seen use.

The Markov chain model analyzes the land use zoning images, and the results are an output image and a possible change matrix based on the last year's potential change matrix (Bose and Chowdhury 2020; Salem et al. 2021). The probability of future land use changes is displayed in a change matrix. The bottom-up Markov chain and cellular automata model is a practical simulation method for studying land use shifts. As a geographical model that predicts the future based on identifying the dynamics of complex systems and is user-friendly for LULC forecasting. In addition, it is recognized as a proper two-dimensional method of presenting the spatial and temporal dynamics of location (Shao et al. 2019; Mondal et al. 2022). Markov models are effective in tropical and subtropical regions and on various scales (Ziyad Ahmed Abdo 2020). Recent advances in RS and GIS have led to greater precision in computation and modeling (Abdullahi and Pradhan 2018).

In this study, we proposed the use of CA–Markov model, which combines Cellular Automata and Markov chains to simulate hypothetical situations. It is common practice to utilize a Markov chain model to calculate the transition probabilities among several land cover categories at a given time. A CA model is then used for these probabilities to make time-dependent, spatially explicit predictions. A CA–Markov model's foundation is an initial distribution and transition matrix, which together assume that the drivers that produce the observed patterns of land cover categories will continue to act in the future as they have in the past (Al-Najjar et al. 2019; Prasad et al. 2022; da Silva Monteiro et al. 2022). A CA–Markov model is suitable for a counterfactual approach because it allows us to extrapolate the landscape before intervention into the future while assuming that the type of intervention will remain the same (Arnfield 2003).

In this research, we examine the past and present to predict the future of LULC in Peshawar districts. Natural resources become a major problem because of this region's significant concentration of forestation and deforestation activities (KPK). This research aims to create a model of every LULC in our study region by combining cellular automata and Markov chain. The structure of this paper is as follows. For more precise simulations in 2022, 2038, and 2054, see the “[Material and methods](#)” section, where data is prepared from the LULC map between 1990 and 2022. This map will be used in conjunction with the Markov model. The “[Results](#)” section provides an overview of the technique, tools, software, and support for the Markov model and cellular automata hybrid. The “[Discussion](#)” section would review the results of our CA–Markov model simulation covering

2022 through 2054 and several possible application methods. The “[Conclusion](#)” section would discuss our results with data limitations, a brief overview of our findings, and some suggestions for future research.

## Material and methods

### Study area

Peshawar, a major city in eastern Khyber Pakhtunkhwa (KPK), is one of Pakistan’s oldest and largest administrative centers. Located at 33° 41’–34° 12’ N and 71° 27’–71° 47’ E, Peshawar has a total land area of around 1264 square miles (Fig. 1) (Mumtaz et al. 2020; Ahmad et al. 2021). Winter officially begins in November and lasts until March. The summer season lasts from the beginning of May through the end of September. The local economy benefits from the production of agricultural goods, manufactured goods, and

industrial goods. It serves as the nerve center for the province’s economy, as well as for its schools and other public institutions. In the most recent census, taken place in 1998, the urban population of Peshawar made up 33% of the total population (Tariq et al. 2022a). The inflow of Afghan migrants initiated rapid urbanization in Peshawar after 1978, which continued until the 1998 census. The people would not have reached 2.01 million without the influx of Afghan refugees. It also appears to be related to the yearly growth rate of 4% between 1998 and 2017, while the sex ratio is 106.5. Commercial activity is essential to the city’s development (Baqa et al. 2021a).

### Modeling framework

This section will discuss the primary components utilized for the following land cover alterations. The procedure occurs within a raster data environment, typically a grid of uniform cells with a predetermined resolution. The steps

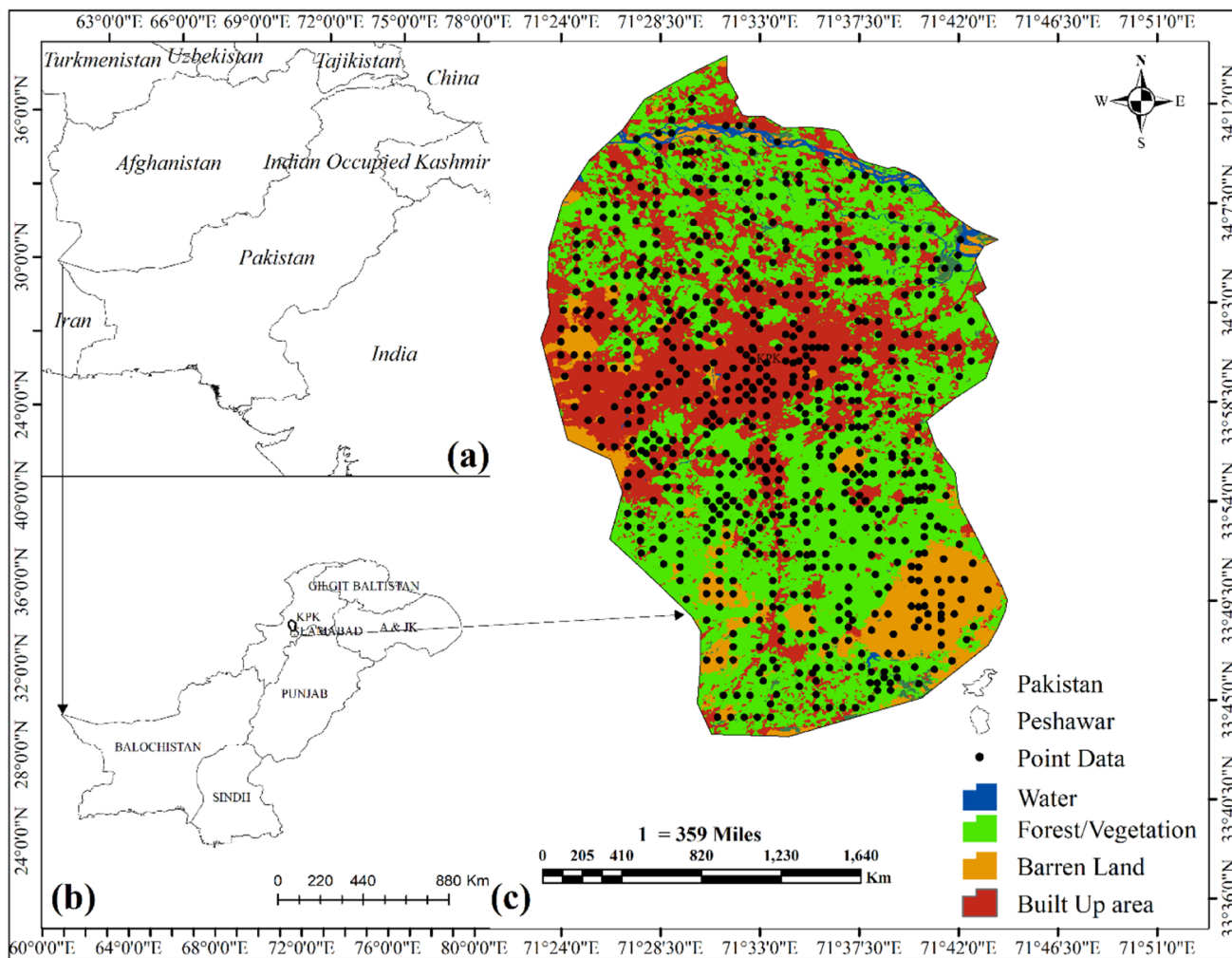


Fig. 1 The geographical location of the study area

taken to complete this research are as follows: (1) classifying satellite images to create land cover maps for 1990, 2006, and 2022; (2) computing a Markov process-derived transition area matrix that indicates the number of pixels expected to change from one land cover class to another over a given period (1990–2006, 2006–2022); (3) obtaining transition suitability images using a Markov chain and a multi-criteria evaluation (MCE) model; (4) Finally, we simulate land cover changes to the year 2038 and 2054 using the CA-Markov module, and (5) assess the model's accuracy by contrasting the difference between the current and projected 2022 maps.

### Data preparation for LULC change analysis

In this investigation, Google Earth Engine was utilized to scan satellite data for images that could provide light on the causes of LULC changes. Landsat images, including those gathered from the actual two satellites observed from 1990 to 2022, were used because of their high spectral and geographic resolution, capacity to alter the topography, and accessibility. Multispectral remote sensing imagery from the USGS's Landsat series, with a 30 by 30 m spatial resolution, was downloaded for the Peshawar district from their website (<https://ers.cr.usgs.gov/>) (Table 1).

### Land cover mapping

Landsat TM, ETM+, and OLI/TIRS images (<https://earthexplorer.usgs.gov/>) were amassed to span 1990–2022. These land cover maps for 1990, 2006, and 2022 were created using Landsat imagery. All images underwent pre-processing techniques (geometric and atmospheric) to eliminate the gaps, fills, and errors created during the imaging process. The land cover maps were created using a classification technique

**Table 1** Satellite images used for LULC classification in this study

S. no.	Row	Path	Year	Date	Sensor
1	151	36/37	1990	08 <sup>th</sup> June	TM
2	151	36/37	2006	13 <sup>th</sup> May	ETM+
3	151	36/37	2022	29 <sup>th</sup> May	OLI/TIRS

**Table 2** Distinct classifications of land use and land cover

S. no.	Class name	Description
1	Built-up areas	Business district, industrial zone, transit corridor, built-up area, residential area, etc
2	Wetland/water bodies	All kinds of waterways: streams, lakes, canals, rivers, ponds, etc
3	Forests	A forest consists of a vast, tree-covered region of land. A group of trees can be called a "forest" as well
4	Vegetation	Lands used for growing crops, forestry, farming, greenhouses, etc
5	Barren land	Material such as rocks, soil, grassland, and so forth

called object-based support vector machine (SVM) after undergoing geometric and atmospheric modifications (Frey et al. 2013; Rodrigues et al. 2018). The so-called salt-and-pepper effect, which typically occurs with pixel-based remote sensing classification systems, can be avoided with the object-oriented classification method. Therefore, there are five broad categories: built-up area, water, forests, vegetation/agriculture, and barren land (Table 2).

### Generating transition area matrix

This research computed the transition area matrices of land cover types for two-time intervals (from 1990 to 2006 and from 2006 to 2022). Each matrix keeps track of how many pixels are classified as belonging to one set but is forecast to change to another set over time. Past trends are used in this model section to estimate how another replaces one class. The Markov chain model is used to produce these matrices, and a 0.1% error in proportion is allowed (Kasischke et al. 2007; Das et al. 2021). By superimposing the 1990 and 2006 categories and outlining the shift between the two eras one class at a time, we generated the 2022 transition area matrices. This data is fed into a Markov model to help predict whether or not a given set of pixels could change from one land cover class (e.g., forest) to another (e.g., field).

### Generating potential transition maps

Creating appropriate maps for different land cover types is challenging because of the need for more relevant data and knowledge. While all the potential influences and limitations of the area under investigation should be considered, this seems unattainable. This study used GIS techniques, MCE, and fuzzy membership functions to extract potential transition maps of land cover categories (Sayemuzzaman and Jha 2014; Zhang et al. 2021). First, possible transition maps of the built-up area, water, forests, vegetation, and barren land environments were computed using two drivers: A conditional probability map with neighborhood interaction (Euclidean distance to cells of the same type). By and large, the probability of a pixel changing into a particular land cover class increases the closer it is to that class it is.

Given that this rule does not hold in all cases (Baqa et al. 2021b; Tariq et al. 2022b), conditional probability images are utilized to lessen the amount of guesswork involved in constructing potential transition maps. As the name implies, dependent probability images depict the likelihood that each pixel in the subsequent period will fall into the specified class based on its current state. Thus, the images above represent a graphical depiction of the matrix of transition probabilities (Halmy et al. 2015; Baqa et al. 2021a). There were limits on built-up areas, water, forests, vegetation, and barren land due to cities and bodies of water. And therefore, to create a transition potential map of urban regions, we settled on four fundamental biophysical and proximal drivers: neighborhood interaction, distances from water bodies, distance from the nearest road, and slope (Table 3). Water bodies are also included in the zone where development is prohibited. Research has demonstrated that these extraneous details strongly correlate with the likelihood of urban transformations (Tariq and Shu 2020; Munthali et al. 2020).

Since the Markov chain cannot pinpoint where precisely land cover changes occur, we used GIS methods, MCE, and fuzzy membership functions to zero in the most promising areas for change. Fuzzy sets provide a consistent metric without requiring arbitrary Boolean constraints or thresholds to be determined in advance (Arsanjani et al. 2013). To re-scale driver maps from  $-128$  to  $+128$ , where  $-128$  represents the least suitable sites, and  $+128$  represents the most relevant sites, fuzzy membership functions (such as the sigmoidal monotonic decline function) were employed. Moreover, MCE's analytic hierarchy process (AHP) was used to provide relatively important ratings to each of the MCE's contributing variables (Fu et al. 2018). The AHP technique incorporates growth limits and permits weighing land cover transition potential based on a set of potential maps (for example, slope magnitude). The AHP provides a thorough and reasonable framework for resolving the choice problem by identifying and measuring its components, establishing links between them and the overarching goals, and evaluating potential courses of action. Because of

its flexibility in incorporating a wide range of heterogeneous factors and its ease in determining appropriate weights for those variables, this GIS-based AHP is a potent instrument (Behera et al. 2012; Yulianto et al. 2019). This model sparkles when crucial variables are hard to quantify and compare or when it is challenging to build communications between team members due to their different areas of expertise, and opinions.

## Model evaluation

Even though evaluating a model is crucial, there is currently no agreed-upon standard to measure how well a landscape change model performs (Baqa et al. 2021b). The model is tested to see if it produces an unexpected land cover map projection. It is common practice to compare the results of a model's simulation to the world as it exists to verify the model's accuracy. Similar methods have been favored in other research, such as (Arsanjani et al. 2012), who used them to validate a model forecasting land cover change. Kappa variation statistics were used to compare the observed transitions between the satellite images from 1990 and 2022 with the projected map of 2022 produced from remote sensing techniques. The kappa index is a widely used and respected metric for comparing maps (Tariq and Shu 2020). Kappa statistics evaluate the model's performance regarding the percentage of correctly categorized cells and their precise locations.

Here, we introduce three kappa statistics:

- The standard kappa ( $K_{\text{standard}}$ ), which measures the simulated layers' ability to achieve perfect classification.
- A modified general statistic over ( $K_{\text{standard}}$ ), ( $K_{\text{no}}$ ), which displays the fraction of pixels correctly classified relative to the expected fraction of pixels correctly classified without the ability to specify quantity or location.
- A ( $K_{\text{location}A}$ ) index that can distinguish the locational accuracy of pixels in the similarity layer.

**Table 3** Calculated values for urban regions using AHP and fuzzy standardization

S. no.	Factors	Functions	Control points	Weights
1	Distance from roads	J-shaped	0–25 m highest suitability 25–100 m decreasing suitability > 100 m no suitability	0.28
2	Distance from water bodies	Linear	0–50 m no suitability 50–500 m increasing suitability > 500 m highest suitability	0.15
3	Distance from built-up areas	Linear	0–50 m highest suitability 50–100 km decreasing suitability > 100 km no suitability	0.38
4	Slope	Sigmoid	0–10% highest suitability 10–25% decreasing suitability > 25% no suitability	0.19

It can go from 0 (an utterly arbitrary place) to 1 (a perfectly specified position) (Aburas et al. 2017).

## CA–Markov model

When it comes to modeling, CA-Markov modeling is a hybrid approach that combines the best features of deterministic, spatially explicit models with the flexibility and adaptability of stochastic, temporal models. This model, which is a hybrid of Markov chains and CA models, has proven to be an effective tool for simulating dynamic spatial phenomena and predicting land cover changes over time and space, both from the perspective of existing conditions and that of any additional factors that may influence transitions among land cover classes in the future. Recalibrating the supporting data with these findings can then be used for theoretical constructions and scenario-based projections. When the causes and effects of land cover changes are unclear, a Markov chain is an effective model for forecasting land change demand (Fan et al. 2008).

In this approach, we can predict environmental outcomes by looking only at historical data. The Markov chain model is a stochastic process model used to represent the probabilities of transitions between states and make predictions. Creating a transition probability matrix of land cover change across time allows for this, as it indicates that the changes may still be utilized to anticipate the following period. Each transition probability is displayed in this model, but the spatial distribution of these events is left unexplored. As a result, the CA is applied to spatial personalities. In the CA model, each lattice cell can exist in one of a fixed number of states. These states persist indefinitely or evolve into new forms with each iteration or time step (Ahmed and Ahmed 2012). A collection of deterministic rules is defined in advance of the execution of this process, and those rules are what spark the necessary adjustments. Running CA requires four parameters: (1) a cellular (or grid) space, (2) a neighborhood specification, (3) a fixed number of states, and (4) a set of transition rules. The power of CA lies in its ability to accurately model processes that unfold in both artificial and natural systems over time and place. This makes them an excellent tool for investigating the dynamics of complex systems (Radwan et al. 2019). The spatial dynamics are managed by CA's local transition rules, while the temporal dynamics of land cover classes are represented by Markov processes based on transition probabilities (Ahmed and Ahmed 2012).

In a multi-object land allocation procedure, the suitability images are combined with the base land cover and the transition matrices to generate future land cover maps. All pixels are evaluated for their potential use in each land cover category. At any given time in the simulation, several land cover types may occupy any given pixel (except by restricted

and unchangeable areas) (Fan et al. 2008). Considering the predetermined spatial limitations of the CA and the temporal step to be classified for the given period, the class with the highest appropriateness at that pixel will be selected. For each category of land use, the procedure is carried out, and it is repeated multiple times for each time interval. Total number of pixels in each land cover class is determined by first eliminating the least likely pixels from inclusion in that class (Arsanjani et al. 2012). Due to the inherent uncertainty in the procedure, we iterated over multiple iterations to generate the possible land cover class for each period. Multiple runs of this method were combined into a frequency image to determine which regions are more likely to be another region. This image was created by superimposing all the simulations for a specific land cover type over a specific period (Radwan et al. 2019). It reveals the frequency with which each cell was assigned to a specific land cover type. This study's methodology is depicted in Fig. 2. Below is a flowchart explaining the process in greater depth.

## Results

### Land cover classification and accuracy assessment

An object-oriented approach was taken to image processing to create a multi-temporal land cover geographic database for the three years of analysis. The estimated categorization accuracy allowed the resulting maps to be used for additional change analysis. We collected ground truth data (training and validation data) from Quickbird images hosted on Google Earth (<http://earth.google.com>) to evaluate the precision of classified images. After collecting a random sample of ground truth points from the region covered by high-resolution Quickbird images. We superimposed those points on the images in Google Earth and used visual interpretation to categorize them into appropriate groups for the entire research area. If land cover patches covered at least one Landsat pixel, that location was assigned to a distinct category (30 × 30m). The training locations were precisely chosen and limited to homogenous regions whose class membership was consistent between 1990 and 2022 based on human interpretation of Landsat imagery. We reached the highest possible, stable accuracy by fine-tuning the training sample dataset. This optimization process involved erasing training data that could have contributed to errors or adding fresh samples to incorrectly labeled categories. We mapped 1374 points using a sample taken from Quickbird images. We separated all ground truth points into training (70%) and testing (30%) data. The overall accuracy of the extracted land cover maps for 1990, 2006, and 2022 ranged between 89.02% and 94.02%, proving the usefulness of the classified remote sensing images for accurate and efficient land

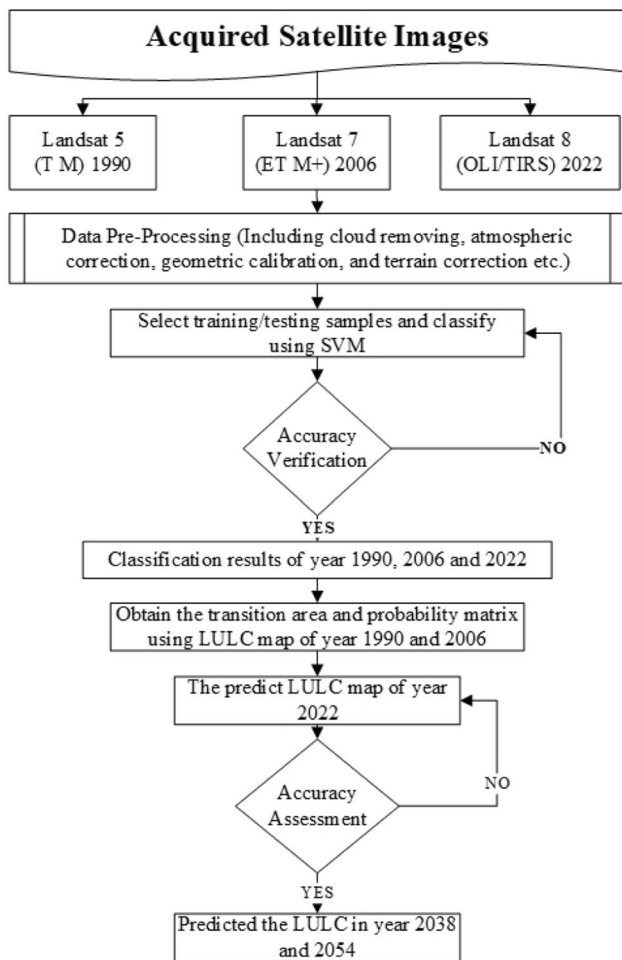


Fig. 2 General description of the methodology

cover change analysis and modeling (Table 4). As a result, we could create land cover maps for the whole research area using 100% ground truth data. The finished land cover maps are shown in Fig. 3.

**Analysis of landscape metrics**

Table 5 shows a breakdown of land cover area changes from 1990 – 2022, which shows that the %age of land

covered by buildings increased from 5.81% to 17.33%. Between 1990 and 2006, over 73.51 km<sup>2</sup> was developed, and between 2006 and 2022, another 145.64 km<sup>2</sup> is expected to be built upon. There was a steady growth in developed areas and a corresponding decline in the agricultural, forested, and barren land. Between 1990 and 2022, barren land decreased dramatically, from 380.25 km<sup>2</sup>(30.08) to 203.12 km<sup>2</sup> (16.06%). During this era, forest area dropped from 312.25 km<sup>2</sup> (24.70) to 191.08 km<sup>2</sup> (15.11). Furthermore, the percentage of vegetation in 1990 increased by 485.10 km<sup>2</sup> (38.38%) to 552.36 km<sup>2</sup> (43.69%) in 2022. Some more water has been added to the landscape.

**Analysis of the transition matrix**

Before the final CA–Markov model was created, the transition matrices were generated by the Markov model provided information on the amount of change and the likelihood of change. Here, we see how each land cover will likely evolve over the next few years using transition potentials based on data from 1990 to 2006 and 2006–2022. Total land areas, as determined by the categories, were compared to the transition area matrices. The probability of change from one phenomenon to another can be calculated using transition probability matrices (Table 6). The on-diagonal statistics show how likely a phenomenon will continue as before, while the off-diagonal data show how likely the sensation will change (Tariq and Shu 2020). The Markov transition probability matrix indicates that between 1990 and 2006, there is a 13.3% chance of the forest transitioning into the forest. The likelihood of a shift in this direction dropped to a reasonable 10.9% in 2022. According to Table 6, barren land and vegetation areas had the highest probability of urbanization during both epochs. Over the two time periods, there was an upward trend in the likelihood of staying in the same class. Between the two estimates, water bodies saw the most growth. It is estimated that after ten years, 96% of water pixels will still be water, and after 20 years, that number rises to 98%.

**Table 4** Accuracy assessment derived by satellite images; (a) 1990, (b) 2006, and (c) 2022

LULU	1990				2006				2022			
	UA	PA	OA	K	UA	PA	OA	K	UA	PA	OA	K
Built-up area	94.00	94.00	93.60	0.88	94.00	94.00	94.02	0.87	88.00	97.78	91.02	0.86
Water	92.00	97.87			96.00	94.12			90.00	86.54		
Forests	94.00	88.68			94.00	90.38			92.00	88.46		
Vegetation	96.00	92.31			90.20	95.83			88.00	83.02		
Barren Land	92.00	95.83			96.00	96.00			88.00	91.67		

UA, user’s accuracy; PA, producer accuracy; OA, overall accuracy; K, kappa coefficient

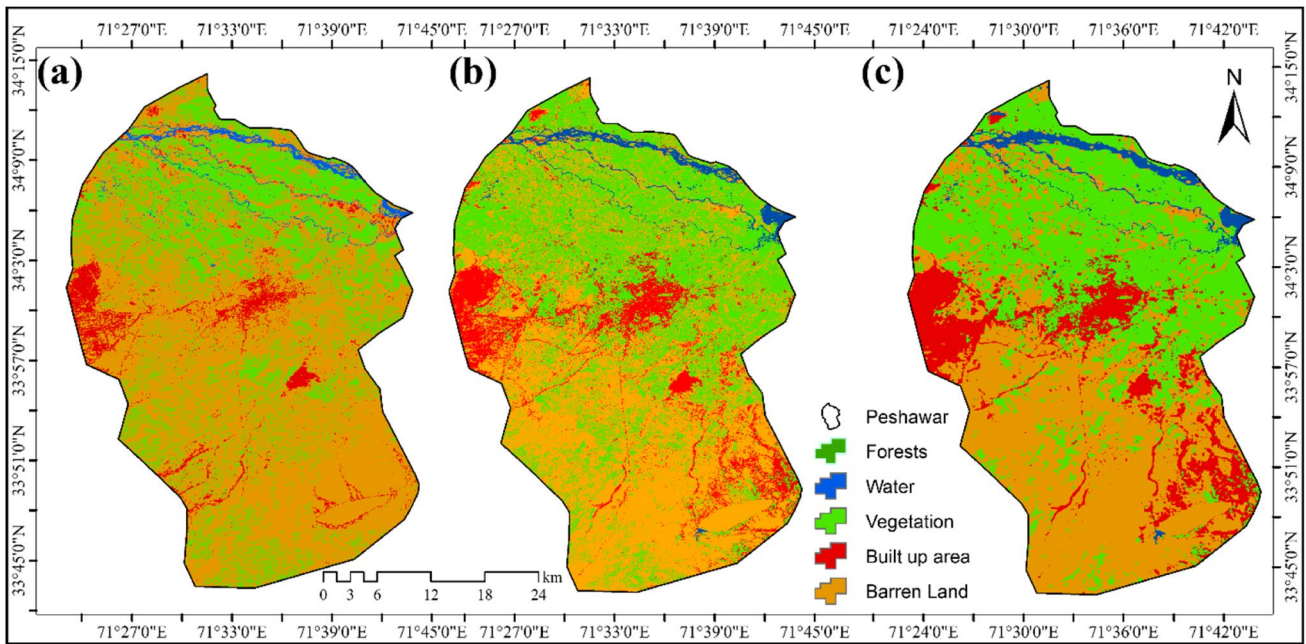


**Fig. 3** Time series of land cover maps; **a** 1990, **b** 2006, and **c** 2022

**Table 5** Changing land cover types and their %age contributions from 1990 to 2022

LULU	Years			Change in land cover structure		
	1990 (%)	2006 (%)	2022 (%)	1990–2006 (%)	2006–2022 (%)	1990–2022 (%)
Built-up area	66.53 (5.26)	140.04 (11.08)	285.68 (22.59)	73.51 (5.81)	145.64 (11.52)	219.15 (17.33)
water	20.13 (1.59)	28.15 (2.23)	32.15 (2.54)	8.02 (0.63)	4.00 (0.32)	12.02 (0.95)
Forests	312.25 (24.70)	298.52 (23.61)	191.08 (15.11)	– 13.73 (– 1.09)	– 107.44 (– 8.50)	– 121.17 (– 9.59)
Vegetation	485.10 (38.37)	365.32 (28.90)	552.36 (43.69)	– 119.78 (– 9.47)	187.04 (14.79)	67.26 (5.32)
Barren land	380.25 (30.08)	432.25 (34.19)	203.12 (16.06)	52.00 (4.11)	– 229.13 (– 18.12)	– 177.13 (– 14.01)

**Table 6** Land cover transition probabilities from 1990 to 2006 and 2006–2022

LULU	Built-up area	Water	Forests	Vegetation	Barren land
1990–2006					
Built-up area	0.9456	0.0087	0.0192	0.0245	0.0071
Water	0.0105	0.9841	0.0415	0.0745	0.0241
Forests	0.0047	0.0215	0.9123	0.0041	0.0152
Vegetation	0.0211	0.0145	0.0174	0.8451	0.0641
Barren land	0.0154	0.0561	0.0891	0.0057	0.8841
2006–2022					
Built-up area	0.9254	0.0654	0.0341	0.0045	0.0003
Water	0.0094	0.9643	0.007	0.1221	0.0065
Forests	0.0107	0.0241	0.9076	0.0475	0.0145
Vegetation	0.0496	0.0424	0.0122	0.7982	0.0003
Barren land	0.0135	0.0083	0.0051	0.0017	0.9715

## Landover modeling and validation

Model performance was measured by contrasting a generated map from 2022 with the actual land cover map from 2022 using kappa modifications. Figure 4 displays the relative error of less than 3% for five types of land cover change between observations and simulations for 2022.

Models with 80% or higher accuracy are regarded as powerful forecasting tools (Tariq et al. 2022b). The  $K$  expected value of 91.2% confirmed this model's correctness. According to (Arsanjani et al. 2013), the  $K_{no}$  value is preferable to the standard when evaluating the model's precision. Overall, the model did a great job of predicting the land cover map in 2022 ( $K_{no}$  = 89.1%), and the result of 93.2% for location shows that the model gives a decent demonstration of the locations in question. Visual analysis of the results (Fig. 5) also reveals a striking similarity between the actual and hypothetical 2022 maps. This means that the kappa values can be used to predict how the land will look in the future using the CA–Markov model.

## Analysis of simulation results

Our findings show that by 2054, the percentage of the study area covered by built-up areas would have increased from 22.59% in 2022 to 30.34%, while the percentage of all other land cover categories (other than the vegetation and water class) would have decreased (Table 7). Forest, for instance,

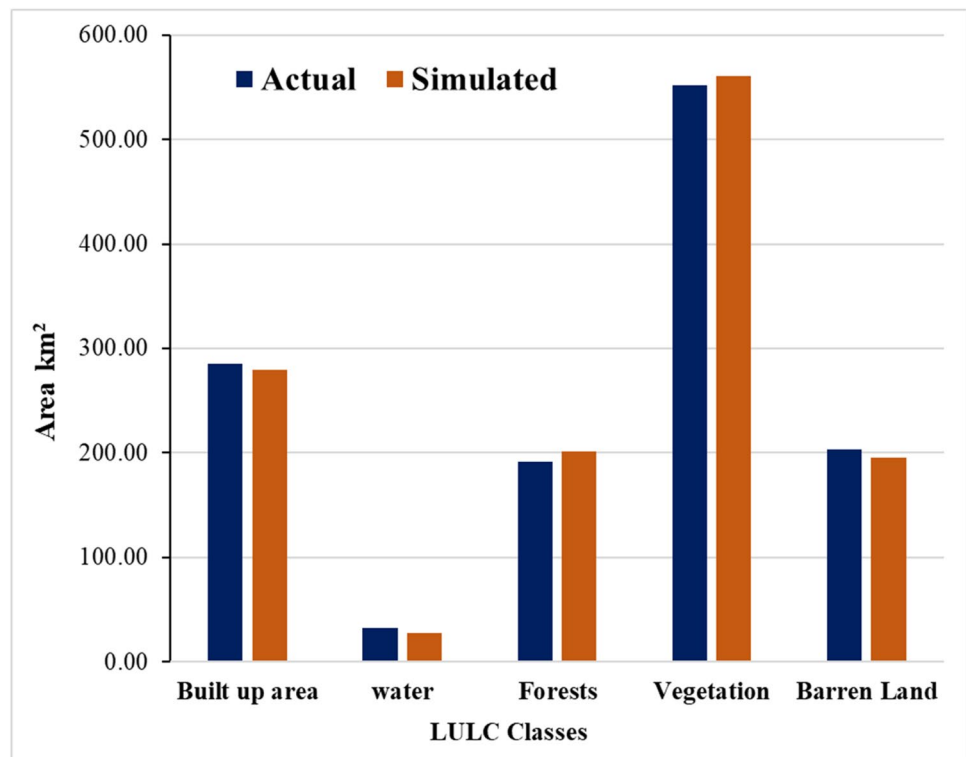
decreased from 191.08 km<sup>2</sup> (15.11%) to 151.76 km<sup>2</sup> (12%) between 2022 and 2054. Vegetation area increased from 552.36 km<sup>2</sup> (43.69%) to 578.60 km<sup>2</sup> (45.77%), while barren land area decreased from 203.12 km<sup>2</sup> (16.06%) to 110.03 km<sup>2</sup> (8.70%) over the same period.

## Discussion

This study used GIS and multi-temporal remote sensing data to examine land cover changes from 1990 to 2006, 2006 to 2022, and 2022 to 2054. From 1990 to 2022, our data shows that the amount of land covered by buildings increased by 17.33%. In this period, developed land has expanded by 219.15 km<sup>2</sup>. This indicates that there has been rapid growth in urban and rural areas over the previous three decades. Therefore an increase in the latter could be interpreted as a loss in the former (nature land = total land area minus (farmland area minus built-up area (Fu et al. 2018). According to Table 4, between 1990 and 2022, the amount of land devoted to nature rise from 66.53 to 285.68 km<sup>2</sup>. For instance, forest cover decreased by 312.25 to 191.08 km<sup>2</sup> between 1990 and 2022. The widespread degradation and destruction of natural and semi-natural areas are a significant problem that spans nearly all Western and Central Europe (Halmy et al. 2015; Zhang et al. 2021).

According to this research, forest land lost a higher proportion of its area than barren land between 1990 and

**Fig. 4** Simulated and actual LULC types for the year 2022



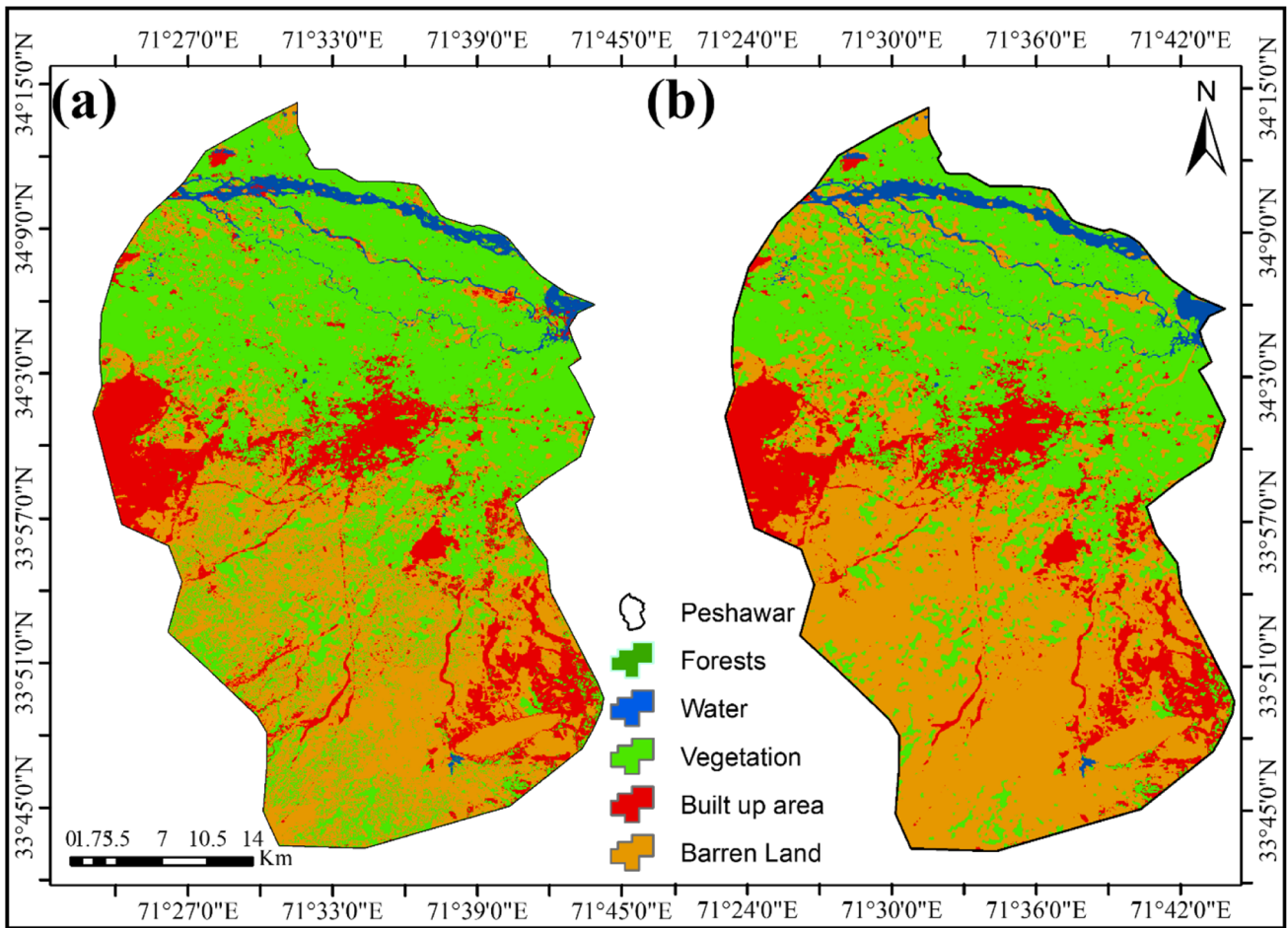


Fig. 5 a Simulated map, b actual map of LULC types in 2022

**Table 7** Absolute quantities for LULC types in km<sup>2</sup> (%) for 2022–2054

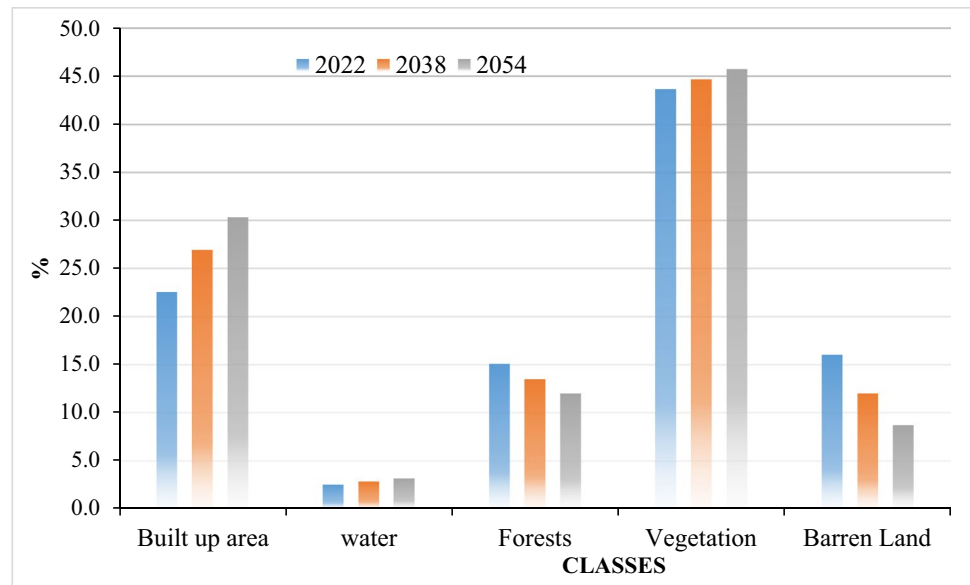
LULU	Land cover classes (km <sup>2</sup> )					
	2022	%	2038	%	2054	%
Built-up area	285.68	22.59	340.54	26.94	383.54	30.34
Water	32.15	2.54	36.15	2.86	40.23	3.18
Forests	191.08	15.11	170.52	13.49	151.76	12.00
Vegetation	552.36	43.69	565.01	44.69	578.60	45.77
Barren land	203.12	16.06	152.03	12.03	110.03	8.70

2022. Table 4 reveals that barren land has decreased 380.25 km<sup>2</sup> of their acreage. Forests in Pakistan were shown to be highly vulnerable, as predicted by these findings. Previous research has warned that forest degradation could severely affect ecosystem services (such as the carbon cycle, regional economics, and climate) (Ahmed and Ahmed 2012; Radwan et al. 2019). However, forests are declining in our study area. Although forests are home to more than half of the vascular plant species in Pakistan (Alexakis et al. 2014), the Pakistan Forest Department notes that only 4% of forests in Pakistan (Mosammam et al. 2017). This led to a significant

reduction in forest acreage. Deforestation rates, however, have begun to fall due to new national and regional initiatives (Hou et al. 2019). Deforestation in the second decade of this study (2006–2022) was nearly half (0.58) of the first decade of this study (1990–2006). In contrast, a downward trend increased in the forest, causing this area to decrease by roughly 1.72 times greater than in the first decade.

The results of the area change shown in Fig. 6 indicate that the area of urbanized regions will expand by 2054. In the next few years, we expect an increase of around 383.54 km<sup>2</sup> in the developed regions. As seen in Fig. 7, the findings

**Fig. 6** Area change of land cover classes from 2022 to 2054



of the spatial distribution show that all land cover classes will show concentrated spatial distribution patterns, with urban built-up land expanding to suburban areas and vegetation in the suburbs quickly converting into built-up land.

Overall, CA–Markov model results pointed to a decline in ecologically significant land. In 2054, vegetation is forecast to cover 45.77% of our research region, a drop of 43.69% from its current distribution. These findings elucidated the seriousness of habitat loss and landscape fragmentation in the research area, both of which can disrupt habitat connectivity and lead to a landscape mosaic of appropriate, less suitable, and unsuitable habitat patches for species (Mumtaz et al. 2020). The emergence of fewer optimal environments for species establishment may enhance competition among species. The rate at which different species migrate from one location to another is predicted to be slow considerably due to competition (Hu et al. 2021; Wahla et al. 2022). Some endangered species may go extinct because of rising levels of competition and falling rates of emigration. According to previous research (Abdullahi and Pradhan 2018; Munthali et al. 2020; Majeed et al. 2022), landscape changes will play a significant influence in limiting the distribution areas of species in the following decades, especially at a local scale (Sayemuzzaman and Jha 2014) like our study area.

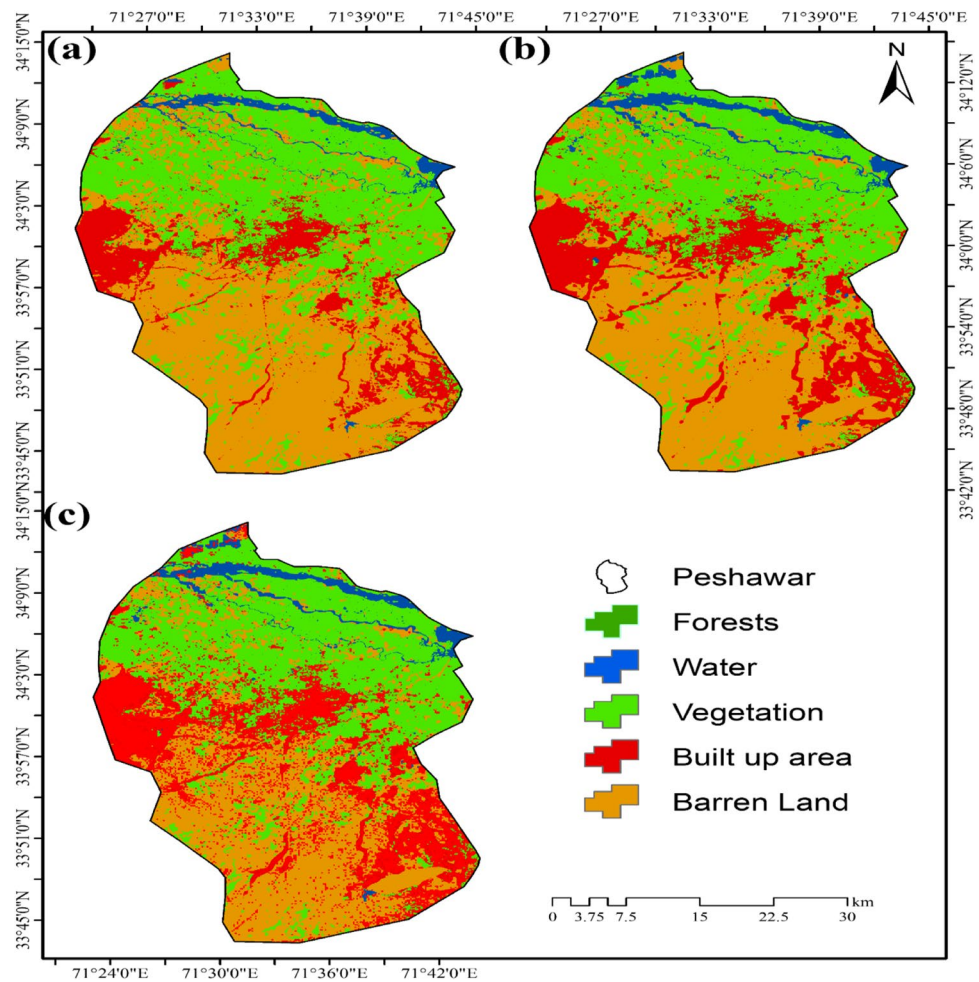
Even though the model employed in this work has shown excellent simulated performance, there are still several unknowns in future estimations of land cover classes. Before anything else, it is worth noting that the land cover maps from 2022, both actual and simulated, show some noticeable changes. Results from LULC classification will indeed affect the realism of simulated land cover changes (Arsanjani et al. 2013). The categorized images are only partially accurate, even though object-based SVM is a highly effective

classification method for dealing with complex class distributions (Fu et al. 2018; Yulianto et al. 2019). This misclassification may be considered uncertainty in such research.

Second, numerous publications have criticized the form of the contiguity filter employed in this work as an additional source of uncertainty, as well as the need for suitable suitability maps for modeling the land cover classes (Behera et al. 2012). The realism of the simulated landscapes is significantly affected by the suitability maps employed in this research. They serve as guidelines for modeling, which is why they are so important. The guidelines derived from the various suitability maps might have wildly diverse impacts. Additional study is needed to see how the forecasts change when the suitability maps are modified.

Third, while this research did indicate that the Markov chain analysis process is an efficient way to determine the transition probability of landcover classes, the analysis relied on the assumption that these probabilities would remain constant over time. In other words, this model's projected future changes in land cover are constructed from existing land cover patterns. Because the model cannot evaluate the novel processes on land cover structures, this problem introduces uncertainty in modeling land cover changes. Our findings, for instance, reveal that the probability of a given land type's transformation into an urban area during the period 1990 – 2022, and the subsequent land changes modeled based on this data, was relatively high. A new urban planning methodology, critical reconstruction, was thus applied in these regions (Arsanjani et al. 2012; Aburas et al. 2017). After 1990, this policy's execution resulted in the rapid transformation of numerous rural areas (including agricultural lands) into new industrial and urban centers (Fan et al. 2008). This meant that in

**Fig. 7** Simulated map of land cover type from 2022 to 2054



the East (including our study area), the likelihood of moving from undeveloped to developed areas was exceptionally high. However, most of these shifts have concluded at this point, and the possibility of further urbanization (the probability of a region becoming developed) is expected to drop dramatically over the next few years.

The SDGs (11 and 15) goal represents sustainable cities and to promote sustainable management of all types of forests by 2022, restore degraded forests, and substantially increase global reforestation. Combined with the actual situation of the study area and the availability of all remote sensing and ancillary data, this study developed SDGs 11 and 15 using the land change transfer map for simplification. Modeling and monitoring the land uses allow decision-makers and residents to visualize and compare the potential impacts of land use change at a neighborhood, community, and regional level. Finally, there is much room for error in predicting how the landscape will change due to natural disasters (like fires and floods), the effects of climate change, changes in managerial perspective, and the inherent uncertainty of using simulation models.

### Conclusion

According to our research findings, combining Geographic Information Systems and Remote Sensing, and land change modeling provides a better understanding of the future potential outcomes and patterns that the landscape may experience. The simulated future land cover maps have the potential to act as an early warning system for comprehending the effects that will be caused by changes in land cover in the future. This is necessary because natural lands are deteriorating. Finally, these important results have implications for land cover planning as a whole. To better balance the growth of urban areas with the preservation of ecological environments, they aid local authorities (policy makers, urban planners, natural resources managers, and land cover management organizations) in better comprehending a complex land cover system and developing improved land cover management. This method should be empirically repeated, and additional comparative research should be conducted to establish whether the

patterns of projected landscape changes are unique to the area that is the focus of our investigation.

**Acknowledgements** We are highly thankful to the unspecified reviewers and journal editors for their enthusiastic support and valuable suggestions during the manuscript review. All the authors would like to thank Miss Sumaira Jamil and Stephen C. McClure for their active support and valuable suggestions during the manuscript review.

**Author contribution** Aqil Tariq conducted the overall analysis and led the writing of the manuscript, design, and data analysis. Faisal Mumtaz lends their support to authors for writing analysis of Landsat data.

**Funding** This study was supported by National Natural Science Foundation of China (grant 41907192) and civil aerospace pre-research project (D040102).

**Data availability** The datasets generated and analyzed during the current study are not publicly available but are available from the corresponding author at a reasonable request.

## Declarations

**Ethics approval and consent to participate** The facts and views in the manuscript are solely ours, and we are responsible for authenticity, validity, and originality. We also declare that this manuscript is our original work and is not copied from anywhere else. No plagiarism is detected in this manuscript.

**Consent for publication** We undertake and agree that the manuscript submitted to your journal has not been published elsewhere and has not been simultaneously submitted to other journals.

**Competing interests** The author declares no competing interests.

## References

- Abdullahi S, Pradhan B (2018) Land use change modeling and the effect of compact city paradigms: integration of GIS-based cellular automata and weights-of-evidence techniques. *Environ Earth Sci* 77:1–15. <https://doi.org/10.1007/s12665-018-7429-z>
- Aburas MM, Ho YM, Ramli MF, Ash'aari ZH (2017) Improving the capability of an integrated CA-Markov model to simulate spatio-temporal urban growth trends using an Analytical Hierarchy Process and Frequency Ratio. *Int J Appl Earth Obs Geoinf* 59:65–78. <https://doi.org/10.1016/j.jag.2017.03.006>
- Ahmad A, Ahmad SR, Gilani H et al (2021) A synthesis of spatial forest assessment studies using remote sensing data and techniques in Pakistan. *Forests* 12:1211. <https://doi.org/10.3390/f12091211>
- Ahmed B, Ahmed R (2012) Modeling urban land cover growth dynamics using multioral satellite images: a case study of Dhaka, Bangladesh. *ISPRS Int J Geo-Information* 1:3–31. <https://doi.org/10.3390/ijgi1010003>
- Al-Najjar HAH, Kalantar B, Pradhan B et al (2019) Land cover classification from fused DSM and UAV images using convolutional neural networks. *Remote Sens* 11:1–18. <https://doi.org/10.3390/rs11121461>
- Alexakis DD, Agapiou A, Tzouvaras M et al (2014) Integrated use of GIS and remote sensing for monitoring landslides in transportation pavements: the case study of Paphos area in Cyprus. *Nat Hazards* 72:119–141. <https://doi.org/10.1007/s11069-013-0770-3>
- Arnfield AJ (2003) Two decades of urban climate research: a review of turbulence, exchanges of energy and water, and the urban heat island. *Int J Climatol* 23:1–26. <https://doi.org/10.1002/joc.859>
- Arsanjani JJ, Helbich M, Kainz W, Boloorani AD (2013) Integration of logistic regression, Markov chain and cellular automata models to simulate urban expansion. *Int J Appl Earth Obs Geoinf* 21:265–275. <https://doi.org/10.1016/j.jag.2011.12.014>
- Arsanjani JJ, Helbich M, Kainz W, Boloorani AD (2012) Integration of logistic regression, Markov chain and cellular automata models to simulate urban expansion. *Int J Appl Earth Obs Geoinf* 21:265–275. <https://doi.org/10.1016/j.jag.2011.12.014>
- Atif I, Mahboob MA, Waheed A (2015) Spatio-temporal mapping and multi-sector damage assessment of 2014 flood in Pakistan using remote sensing and GIS. *Indian J Sci Technol* 8. <https://doi.org/10.17485/ijst/2015/v8i35/76780>
- Baqa MF, Chen F, Lu L et al (2021a) Monitoring and modeling the patterns and trends of urban growth using urban sprawl matrix and CA-Markov model: a case study of Karachi, Pakistan. *Land* 10:700. <https://doi.org/10.3390/land10070700>
- Baqa MF, Chen F, Lu L, et al (2021b) Monitoring and modeling the patterns and trends of urban growth using urban sprawl matrix and CA-Markov model: a case study of Karachi, Pakistan. *Land* 10. <https://doi.org/10.3390/land10070700>
- Behera MD, Borate SN, Panda SN et al (2012) Modelling and analyzing the watershed dynamics using Cellular Automata (CA)-Markov model - a geo-information based approach. *J Earth Syst Sci* 121:1011–1024. <https://doi.org/10.1007/s12040-012-0207-5>
- Bose A, Chowdhury IR (2020) Monitoring and modeling of spatio-temporal urban expansion and land-use/land-cover change using markov chain model: a case study in Siliguri Metropolitan area, West Bengal, India. *Model Earth Syst Environ* 6:2235–2249. <https://doi.org/10.1007/s40808-020-00842-6>
- da Silva Monteiro L, de Oliveira-Júnior JF, Ghaffar B et al (2022) Rainfall in the urban area and its impact on climatology and population growth. *Atmosphere (basel)* 13:1610. <https://doi.org/10.3390/atmos13101610>
- Das N, Mondal P, Sutradhar S, Ghosh R (2021) Assessment of variation of land use/land cover and its impact on land surface temperature of Asansol subdivision. *Egypt J Remote Sens Sp Sci* 24:131–149. <https://doi.org/10.1016/j.ejrs.2020.05.001>
- Erinjery JJ, Singh M, Kent R (2018) Mapping and assessment of vegetation types in the tropical rainforests of the Western Ghats using multispectral Sentinel-2 and SAR Sentinel-1 satellite imagery. *Remote Sens Environ* 216:345–354. <https://doi.org/10.1016/j.rse.2018.07.006>
- Fan F, Wang Y, Wang Z (2008) Temporal and spatial change detecting (1998–2003) and predicting of land use and land cover in Core corridor of Pearl River Delta (China) by using TM and ETM+ images. *Environ Monit Assess* 137:127–147. <https://doi.org/10.1007/s10661-007-9734-y>
- Frey O, Santoro M, Werner CL, Wegmüller U (2013) DEM-based SAR pixel-area estimation for enhanced geocoding refinement and radiometric Normalization. *IEEE Geosci Remote Sens Lett* 10:48–52. <https://doi.org/10.1109/LGRS.2012.2192093>
- Fu X, Wang X, Yang YJ (2018) Deriving suitability factors for CA-Markov land use simulation model based on local historical data. *J Environ Manage* 206:10–19. <https://doi.org/10.1016/j.jenvman.2017.10.012>
- Ghaffar A, Shirazi SA, Parveen N, Minallah M (2013) Use of multi-temporal digital data to monitor LULC changes in Faisalabad-Pakistan. *Pak J Sci* 65:58–62
- Halmy MWA, Gessler PE, Hicke JA, Salem BB (2015) Land use/land cover change detection and prediction in the north-western coastal desert of Egypt using Markov-CA. *Appl Geogr* 63:101–112. <https://doi.org/10.1016/j.apgeog.2015.06.015>

- Hassan Z, Shabbir R, Ahmad SS et al (2016) Dynamics of land use and land cover change (LULCC) using geospatial techniques: a case study of Islamabad Pakistan. *Springerplus* 5:812. <https://doi.org/10.1186/s40064-016-2414-z>
- Hou H, Wang R, Murayama Y (2019) Scenario-based modelling for urban sustainability focusing on changes in cropland under rapid urbanization: a case study of Hangzhou from 1990 to 2035. *Sci Total Environ* 661:422–431. <https://doi.org/10.1016/j.scitotenv.2019.01.208>
- Hu P, Sharifi A, Tahir MN et al (2021) Evaluation of vegetation indices and phenological metrics using time-series modis data for monitoring vegetation change in Punjab, Pakistan. *Water (switzerland)* 13:1–15. <https://doi.org/10.3390/w13182550>
- Hussain S, Qin S, Nasim W et al (2022) Monitoring the dynamic changes in vegetation cover using spatio-temporal remote sensing data from 1984 to 2020. *Atmosphere (basel)* 13:1609. <https://doi.org/10.3390/atmos13101609>
- Kasischke ES, Bourgeau-Chavez LL, Johnstone JF (2007) Assessing spatial and temporal variations in surface soil moisture in fire-disturbed black spruce forests in Interior Alaska using spaceborne synthetic aperture radar imagery — implications for post-fire tree recruitment. *Remote Sens Environ* 108:42–58. <https://doi.org/10.1016/j.rse.2006.10.020>
- Khan TU, Mannan A, Hacker CE, et al (2021) Use of gis and remote sensing data to understand the impacts of land use/land cover changes (Lulcc) on snow leopard (*panthera uncia*) habitat in Pakistan. *Sustain* 13. <https://doi.org/10.3390/su13073590>
- Kim SW, Brown RD (2021) Urban heat island (UHI) intensity and magnitude estimations: a systematic literature review. *Sci Total Environ* 779:146389. <https://doi.org/10.1016/j.scitotenv.2021.146389>
- Li X, Wang Y, Li J, Lei B (2016) Physical and socioeconomic driving forces of land-use and land-cover changes: a case study of Wuhan City, China. *Discret Dyn Nat Soc* 2016. <https://doi.org/10.1155/2016/8061069>
- Li X, Zhou Y, Asrar GR et al (2017) The surface urban heat island response to urban expansion: a panel analysis for the conterminous United States. *Sci Total Environ* 605–606:426–435. <https://doi.org/10.1016/j.scitotenv.2017.06.229>
- Majeed M, Lu L, Haq SM et al (2022) Spatiotemporal distribution patterns of climbers along an abiotic gradient in Jhelum District, Punjab. *Pakistan Forests* 13:1244. <https://doi.org/10.3390/f13081244>
- Mondal BK, Kumari S, Ghosh A, Mishra PK (2022) Transformation and risk assessment of the East Kolkata Wetlands (India) using fuzzy MCDM method and geospatial technology. *Geogr Sustain* 3:191–203. <https://doi.org/10.1016/j.geosus.2022.07.002>
- Morshed SR, Fattah MA (2021) Responses of spatiotemporal vegetative land cover to meteorological changes in Bangladesh. *Remote Sens Appl Soc Environ* 24:100658. <https://doi.org/10.1016/j.rsase.2021.100658>
- Mosammam HM, Nia JT, Khani H et al (2017) Monitoring land use change and measuring urban sprawl based on its spatial forms: the case of Qom city. *Egypt J Remote Sens Sp Sci* 20:103–116. <https://doi.org/10.1016/j.ejrs.2016.08.002>
- Mumtaz F, Tao Y, Leeuw G De, et al (2020) Modeling spatio-temporal land transformation and its associated impacts on land surface temperature (LST). *Remote Sens* 12. <https://doi.org/10.3390/RS12182987>
- Munthali MG, Mustak S, Adeola A et al (2020) Modelling land use and land cover dynamics of Dedza district of Malawi using hybrid Cellular Automata and Markov model. *Remote Sens Appl Soc Environ* 17:100276. <https://doi.org/10.1016/j.rsase.2019.100276>
- Owojori A, Xie H (2003) Landsat image-based LULC changes of San Antonio, Texas using advanced atmospheric correction and object-oriented image analysis approaches. *Area* 1–4
- Prasad P, Joseph V, Chandra P, Kotha M (2022) Ecological Informatics Evaluation and comparison of the earth observing sensors in land cover / land use studies using machine learning algorithms. *Ecol Inform* 68:101522. <https://doi.org/10.1016/j.ecoinf.2021.101522>
- Radwan TM, Blackburn GA, Whyatt JD, Atkinson PM (2019) Dramatic loss of agricultural land due to urban expansion threatens food security in the Nile Delta. *Egypt Remote Sens* 11:1–20. <https://doi.org/10.3390/rs11030332>
- Rodrigues FA, Blasch G, Defourny P, et al (2018) Multi-temporal and spectral analysis of high-resolution hyperspectral airborne imagery for precision agriculture: assessment of wheat grain yield and grain protein content. *Remote Sens* 10. <https://doi.org/10.3390/rs10060930>
- Roy S, Bose A, Majumder S, et al (2022) Evaluating urban environment quality (UEQ) for Class-I Indian city: an integrated RS-GIS based exploratory spatial analysis. *Geocarto Int* 0. <https://doi.org/10.1080/10106049.2022.2153932>
- Roy S, Bose A, Singha N et al (2021) Urban waterlogging risk as an undervalued environmental challenge: an Integrated MCDA-GIS based modeling approach. *Environ Challenges* 4:100194. <https://doi.org/10.1016/j.envc.2021.100194>
- Salem M, Bose A, Bashir B et al (2021) Urban expansion simulation based on various driving factors using a logistic regression model: Delhi as a case study. *Sustain* 13:1–17. <https://doi.org/10.3390/su131910805>
- Samanta S, Pal DK, Palsamanta B (2018) Flood susceptibility analysis through remote sensing, GIS and frequency ratio model. *Appl Water Sci* 8:1–14. <https://doi.org/10.1007/s13201-018-0710-1>
- Sarkar S (2019) Remote sensing based technique for identification of geomorphic features and associated LULC-a case of Chandauli District, Uttar Pradesh (India) Remote Sensing based technique for identification of geomorphic features and associated lulc – a case of Ch. *Int J Res Anal Rev* 5:68–76
- Sayemuzzaman M, Jha MK (2014) Modeling of future land cover land use change in North Carolina using Markov chain and cellular automata model. *Am J Eng Appl Sci* 7:295–306. <https://doi.org/10.3844/ajeassp.2014.295.306>
- Shao Z, Cai J, Fu P et al (2019) Deep learning-based fusion of Landsat-8 and Sentinel-2 images for a harmonized surface reflectance product. *Remote Sens Environ* 235:111425. <https://doi.org/10.1016/j.rse.2019.111425>
- Siddiqui S, Ali Safi MW, Rehman NU, Tariq A (2020) Impact of climate change on land use/land cover of Chakwal District. *Int J Econ Environ Geol* 11:65–68. <https://doi.org/10.46660/ijeege.vol11.iss2.2020.449>
- Tariq A, Mumtaz F, Zeng X et al (2022) Spatio-temporal variation of seasonal heat islands mapping of Pakistan during 2000–2019, using day-time and night-time land surface temperatures MODIS and meteorological stations data. *Remote Sens Appl Soc Environ* 27:100779. <https://doi.org/10.1016/j.rsase.2022.100779>
- Tariq A, Shu H (2020) CA-Markov chain analysis of seasonal land surface temperature and land use landcover change using optical multi-temporal satellite data of Faisalabad, Pakistan. *Remote Sens* 12:1–23. <https://doi.org/10.3390/rs12203402>
- Tariq A, Yan J, Mumtaz F (2022) Land change modeler and CA-Markov chain analysis for land use land cover change using satellite data of Peshawar, Pakistan. *Phys Chem Earth, Parts A/B/C* 1446:103286. <https://doi.org/10.1016/j.pce.2022.103286>
- Tulbure MG, Broich M (2019) Spatiotemporal patterns and effects of climate and land use on surface water extent dynamics in a dryland region with three decades of Landsat satellite data. *Sci Total Environ* 658:1574–1585. <https://doi.org/10.1016/j.scitotenv.2018.11.390>
- Wahla SS, Kazmi JH, Sharifi A, et al (2022) Assessing spatio-temporal mapping and monitoring of climatic variability using SPEI and RF

- machine learning models. *Geocarto Int* 0:1–20. <https://doi.org/10.1080/10106049.2022.2093411>
- Wang S, Ma Q, Ding H, Liang H (2018) Detection of urban expansion and land surface temperature change using multi-temporal landsat images. *Resour Conserv Recycl* 128:526–534. <https://doi.org/10.1016/j.resconrec.2016.05.011>
- Yohannes H, Soromessa T, Argaw M, Dewan A (2021) Impact of landscape pattern changes on hydrological ecosystem services in the Beressa watershed of the Blue Nile Basin in Ethiopia. *Sci Total Environ* 793:148559. <https://doi.org/10.1016/j.scitotenv.2021.148559>
- Yulianto F, Maulana T, Khomarudin MR (2019) Analysis of the dynamics of land use change and its prediction based on the integration of remotely sensed data and CA-Markov model, in the upstream Citarum Watershed, West Java, Indonesia. *Int J Digit Earth* 12:1151–1176. <https://doi.org/10.1080/17538947.2018.1497098>
- Zhang Z, Hu B, Jiang W, Qiu H (2021) Identification and scenario prediction of degree of wetland damage in Guangxi based on the CA-Markov model. *Ecol Indic* 127:107764. <https://doi.org/10.1016/j.ecolind.2021.107764>
- Ziyad Ahmed Abdo SP (2020) A review paper on monitoring environmental consequences of land cover dynamics with the help of geo-informatics technologies. *Geosfera Indones* 5:364–377

**Publisher's note** Springer Nature remains neutral with regard to jurisdictional claims in published maps and institutional affiliations.

Springer Nature or its licensor (e.g. a society or other partner) holds exclusive rights to this article under a publishing agreement with the author(s) or other rightsholder(s); author self-archiving of the accepted manuscript version of this article is solely governed by the terms of such publishing agreement and applicable law.